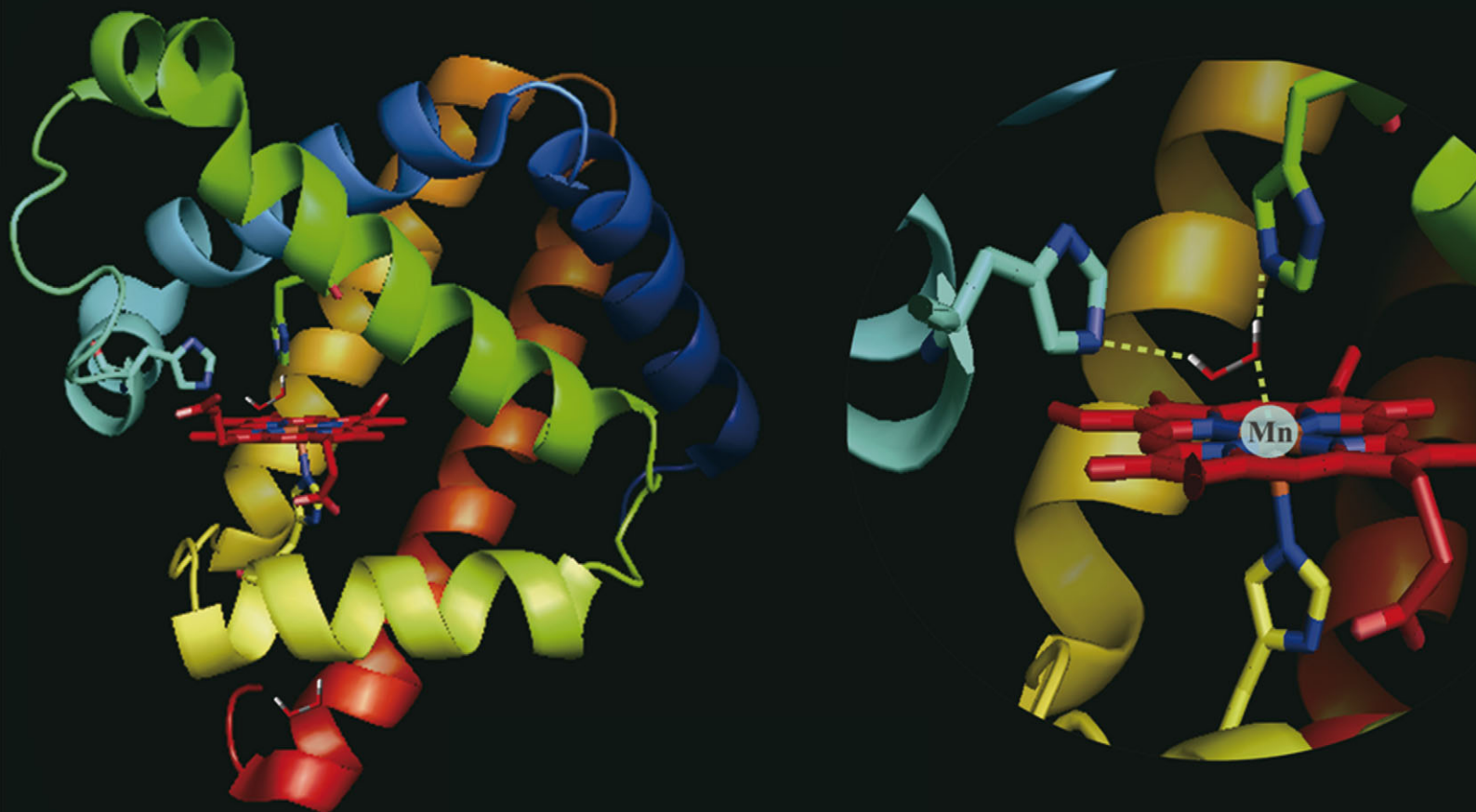


# Metallomics

Integrated biometal science

[www.rsc.org/metallomics](http://www.rsc.org/metallomics)

Volume 5 | Number 7 | July 2013 | Pages 773–938



Themed issue: Metallomics in China

ISSN 1756-5901

RSC Publishing

**PAPER**

Jun-Long Zhang *et al.*  
Effect of distal histidines on hydrogen  
peroxide activation by manganese  
reconstituted myoglobin

**Indexed in  
MEDLINE!**



1756-5901(2013)5:7;1-#

## Effect of distal histidines on hydrogen peroxide activation by manganese reconstituted myoglobin†

Yuan-Bo Cai, Xiao-Han Li, Jing Jing and Jun-Long Zhang\*

Cite this: *Metallomics*, 2013, 5, 828

Myoglobins provide an opportunity to investigate the effect of the secondary coordination sphere on the functionality and reactivity of non-native metal porphyrins inside well-defined protein scaffolds. In this work, we reconstituted myoglobin by the replacement of natural heme with manganese(III) protoporphyrin IX and firstly investigated the effect of distal histidine on the reaction of Mn<sup>III</sup> porphyrin with H<sub>2</sub>O<sub>2</sub> and one-electron oxidation of ABTS. We have prepared L29H, F43H, H64F, L29H/H64F, F43H/H64F, L29H/F43H and L29H/F43H/H64F mutants and reconstituted apo-myoglobins with manganese(III) protoporphyrin IX. Distal histidine at the 64 position plays an essential role in binding H<sub>2</sub>O<sub>2</sub> through hydrogen bond formation, which facilitates the coordination of H<sub>2</sub>O<sub>2</sub> to the Mn center. The second histidine at the 43 position is important in the cleavage of the O–O bond and to form the highly valent Mn(IV)-oxo intermediate. His29 has less efficiency to activate H<sub>2</sub>O<sub>2</sub>, because it is too far from the Mn center. The cooperative effect of dual distal histidines at positions 64 and 43 on the activation of H<sub>2</sub>O<sub>2</sub> was observed and the F43H Mn<sup>III</sup>Mb mutant exhibited 5-fold and 10-fold reaction rate increases in the activation of H<sub>2</sub>O<sub>2</sub> and one-electron oxidation of ABTS *versus* wild-type Mn<sup>III</sup>Mb. This is different from the distal histidine effect on the H<sub>2</sub>O<sub>2</sub> activation by heme in Mb. This work will provide new insights to understand the fundamental chemistry of manganese in oxidation, and further construct biomimetic Mn models for peroxidase, inside or outside of protein scaffolds.

Received 31st December 2012,  
Accepted 15th March 2013

DOI: 10.1039/c3mt20275e

[www.rsc.org/metallomics](http://www.rsc.org/metallomics)

## Introduction

Metalloproteins provide “golden” examples to illustrate the importance of the secondary coordination sphere, previously proposed by Alfred Werner in 1912, to the reactivity of metal centers.<sup>1–7</sup> To understand the secondary coordination sphere inside protein scaffolds, tremendous efforts have been taken to construct models by chemical synthesis as well as biosynthetic approaches.<sup>2,8–13</sup> In particular, the direct utilization of small, stable, easy-to-produce proteins with the characteristic scaffolds as “ligands” to confer the necessary structural features identified in native enzymes attracts considerable attention.<sup>14,15</sup> For example, myoglobins (Mb) have been used as protein scaffolds to mimic heme-containing metalloproteins by site-specific modulation of the proximal and secondary coordination spheres.<sup>16–22</sup>

On the other side, apo-myoglobin (apo-Mb) provides an opportunity to investigate the functionality and reactivity of *non-native metal porphyrins* inside the well-defined protein scaffold. For the similar size, charge and configuration of metal prosthetic groups, manganese, cobalt and other metal protoporphyrin IXs have been employed as non-native metal cofactors through the replacement of the native heme.<sup>23–32</sup> Furthermore, expanding the scope of metal-substituted porphyrins to metal porphyrin-like complexes such as metal salens would enrich the realms of artificial metalloproteins together with the related catalysis. Thus, this approach not only provides new insights to understand the fundamental chemistry of metals in aqueous solution, but also advances the knowledge of their coordination chemistry in biomacromolecules.<sup>33–39</sup>

For the importance of manganese and its redox chemistry in biological systems such as photosystem II,<sup>40,41</sup> bacteria catalases,<sup>42</sup> and mitochondrial superoxide dismutase,<sup>43</sup> the chemistry of highly valent oxo-manganese(IV/V) have been extensively studied. Manganese reconstituted heme proteins such as horseradish peroxidase (Mn<sup>III</sup>HRP),<sup>44–46</sup> cytochrome-c peroxidase (Mn<sup>III</sup>CcP),<sup>47,48</sup> microperoxidase-8 (Mn<sup>III</sup>MP-8),<sup>27,49,50</sup> and myoglobin (Mn<sup>III</sup>Mb)<sup>17,51,52</sup> have been prepared and, through comparative studies with native peroxidases, showed much lower

Beijing National Laboratory for Molecular Sciences, State Key Laboratory of Rare Earth Materials Chemistry and Applications, College of Chemistry and Molecular Engineering, Peking University, Beijing 100871, P. R. China.

E-mail: zhangjunlong@pku.edu.cn; Fax: +86 10-62767034

† Electronic supplementary information (ESI) available: UV-vis spectra of all Mn<sup>III</sup>Mb mutants at pH 5.1. Spectra and kinetic data of reaction with H<sub>2</sub>O<sub>2</sub> at pH 7.4 and 5.1. Spectra and kinetic data of ABTS oxidation at pH 7.4. ESI-MS spectra of all mutants. See DOI: 10.1039/c3mt20275e

reactivity toward hydrogen peroxide. The reactions between  $\text{Mn}^{\text{III}}$  protoporphyrin IX and  $\text{H}_2\text{O}_2$  inside protein scaffolds provided valuable insights for the formation and reactivity of oxo-manganese intermediates in aqueous media. For example, the different ability to form peroxides on iron and manganese centers with  $\text{H}_2\text{O}_2$  could be referred to different  $\text{pK}_{\text{a}}$ s of  $\text{Fe}^{\text{III}}$ MP-8-OH<sub>2</sub> ( $9.2 \pm 0.9$ ) and  $\text{Mn}^{\text{III}}$ MP-8-OH<sub>2</sub> ( $11.2 \pm 0.3$ ),<sup>50</sup> for the similar  $\text{pK}_{\text{a}}$ s of  $\text{H}_2\text{O}$  and  $\text{H}_2\text{O}_2$  (14.0 vs. 12.0, respectively). Thus, pH plays an important role in the deprotonation/protonation of hydrogen peroxide, which is consequently converted to an active oxo-manganese intermediate. This may explain the lower reactivities of manganese reconstituted heme proteins than that of native heme proteins, which is in accordance with previous reports using water-soluble synthetic model porphyrins such as FeTDCPPS and MnTDCPPS.<sup>53–55</sup>

Despite extensive studies on the reactions of manganese porphyrins with  $\text{H}_2\text{O}_2$ , even performed within protein scaffolds, the influence of the secondary coordination sphere has been rarely considered. According to the studies of Wanatabe and coworkers, the distal heme environment affects the reactivity of native heme with  $\text{H}_2\text{O}_2$  significantly.<sup>19,21,22,56–58</sup> The fact that distal histidine relocation mutants (H43F/H64L) increase the reactivity by 11-fold, relative to that of the wild-type Mb, encourages us to investigate the effect of distal ligands around manganese protoporphyrin on the reactivity as peroxidase.

Comparison of crystal structures of myoglobin (Mb) and manganese reconstituted myoglobin ( $\text{Mn}^{\text{III}}$ Mb) led us to propose that Mn protoporphyrin adopts a similar location and coordination sphere to that of native heme inside the Mb scaffold.<sup>17,22,56</sup> Thus, following Wanatabe's work, we chose L29H and F43H as the distal histidine with estimated iron–distal histidine distances of 6.6 and 5.4 Å, respectively.<sup>56</sup> It has been demonstrated that the distance for the F43H mutant is appropriate as a general acid/base. To examine the distal histidine relocation, we chose mutants L29H/H64F and F43H/H64F, for the similar size of phenyl ring to imidazole. To examine the accumulative effect of distal histidine, we chose L29H/F43H, in which three distal histidine are inside the Mb scaffold together with His64. The structures of sperm whale myoglobin (Mb) and the corresponding mutants are shown in Fig. 1. Thus, we investigated how the secondary coordination sphere, especially the hydrogen bond network, affects the reactivity of Mn center. Through reactions of  $\text{Mn}^{\text{III}}$ Mb with  $\text{H}_2\text{O}_2$  (20 equiv.) in pH 7.4, we found that distal environment obviously influence the formation of oxo-manganese(IV) protoporphyrin. His64 is essential for the formation of  $\text{Mn}^{\text{IV}}=\text{O}$ , whereas it is of less importance to form an oxo-iron active intermediate for wild-type Mb. More importantly, the additional distal histidine and its location are important to accelerate the formation rates toward  $\text{H}_2\text{O}_2$ . The F43H  $\text{Mn}^{\text{III}}$ Mb mutant exhibits the highest reaction rate (ca. 5-fold higher than  $\text{Mn}^{\text{III}}$ Mb) among these mutants, whereas L29H decreases the reactivity compared with that of wild type  $\text{Mn}^{\text{III}}$ Mb. An ABTS assay for the peroxidase reactivity of these mutants demonstrated the same trend of distal histidine effect on the formation of the  $\text{Mn}^{\text{IV}}=\text{O}$  intermediate. Thus, in this work, constructing biomimetic Mn models inside the Mb scaffold

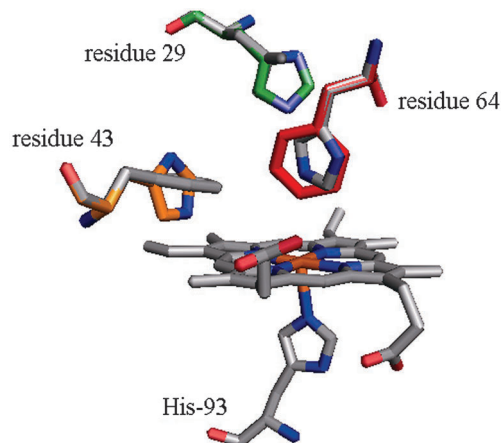


**Fig. 1** Structures of the heme pocket of sperm whale myoglobin (gray). The residues mutated in our studies are also shown: His-29 (green), His-43 (orange), and Phe-64 (red). All N atoms were marked in blue. The PDB code for wild-type Mb is 1JP6. Structures of mutants were reproduced by PyMol.

provides new insights for the secondary coordination sphere effect on the oxidation reactivity of manganese porphyrins in aqueous media.

## Results

### Spectroscopic features of mutated $\text{Mn}^{\text{III}}$ Mb

Computer modelling was used to predict the location of distal histidines in sperm whale myoglobin that would position the Mn protoporphyrin IX cofactor in nearly the same location as the native heme within the protein pocket (PDB: 1JP6, Fig. 1). Residues selected from the model as potential distal points are Leu29, His64, Phe43. Construction, expression, and purification of myoglobin (Mb) with L29H, F43H, H64F, L29H/H64F, F43H/H64F, L29H/F43H and L29H/F43H/H64F mutants were carried out using procedures reported previously.<sup>59</sup> The residues at sites 29, 43, and 64 of these mutants were described in Table 1. The heme in those Mbs was removed by extraction with butanone.<sup>36,60–62</sup> To incorporate Mn protoporphyrin IX into apo-Mbs, 10 equiv. of Mn protoporphyrin in DMSO solution was added to 0.1 mM apo-Mb solution in 50 mM ammonia acetate buffer (pH = 5.1) at room temperature for 1–2 h. According to the previous reports, the evidence for Mn protoporphyrin incorporating apo-Mb was provided by UV/vis spectra of Mn

**Table 1** Residues at site 29, 43, and 64 of wild-type Mb and different mutants

Mutant	Residues		
	Site 29	Site 43	Site 64
Wild-type	Leu	Phe	His
F43H	Leu	His	His
L29H	His	Phe	His
H64F	Leu	Phe	Phe
L29H/F43H	His	His	His
F43H/H64F	Leu	His	Phe
L29H/H64F	His	Phe	Phe
L29H/F43H/H64F	His	His	Phe

protoporphyrin displays two absorption bands at 280 and 376 nm with the ratio of 1:1.8.

Mn<sup>III</sup>Mb and its mutants display characteristic “split” Soret band patterns at  $\lambda_{\text{max}}$  376 and 460–480 nm and Q band at 560–590 nm (Fig. 2a and b). Interestingly, the Soret band at 460–480 nm is sensitive to H64X mutants. Wild-type Mn<sup>III</sup>Mb exhibited an absorption maximum at 471 nm, whereas H64F Mn<sup>III</sup>Mb showed a weaker one with a red shift to 486 nm (Fig. 2a). As reported in Fe<sup>III</sup>Mb, His64 appears to stabilize the heme-bound water, and the loss of water ligation in H64L causes a shift from 408 nm to 393 nm for native heme.<sup>56</sup> In this work, F43H/H64F Mn<sup>III</sup>Mb displays a “split” band at  $\lambda_{\text{max}}$  471 and 483 nm (Fig. 2a) and L29H/H64F Mn<sup>III</sup>Mb displays an absorption at 471 nm (Fig. 2b), blue shifted to that of H64F Mn<sup>III</sup>Mb. The mutants F43H, L29H and L29H/F43H/H64F Mn<sup>III</sup>Mbs, with two distal histidines, showed blue shifts of 466 and 468 nm, respectively, compared to that of wild-type Mn<sup>III</sup>Mb (Fig. 2a and b). According to previous reports, the intensity of the second Soret band component at 486 nm is assigned to the distal-pocket uncoordinated water coordinating

to the Mn<sup>III</sup> ion. From our UV-vis spectra of these mutants, distal histidine plays an important role in controlling water binding to the Mn center and tuning the polarity of the distal environment.

### Reaction of Mn<sup>III</sup>Mb mutants with H<sub>2</sub>O<sub>2</sub>

Since the reaction of wild-type Mn<sup>III</sup>Mb with H<sub>2</sub>O<sub>2</sub> proceeds much slower than that of Fe<sup>III</sup>Mb, the kinetic studies for the formation of the oxo-Mn<sup>IV</sup> species could be carried out by UV-vis spectrophotometer. Wild-type Mb reacted with 20 equiv. H<sub>2</sub>O<sub>2</sub> to yield the Mn<sup>IV</sup>=O species, with a decrease in absorption at 376 nm and 471 nm, and the appearance of a single Soret band at 411 nm. This is similar to Mn<sup>IV</sup>=O hemato-porphyrin IX in MP-8 and Mn<sup>III</sup>HRP (401 and 412 nm, respectively),<sup>44,50</sup> indicating the formation of an Mn<sup>IV</sup>=O species. The reaction also resulted in a nearly isosbestic conversion to Mn<sup>IV</sup>=O and the kinetic trace obeyed pseudo first-order kinetics in the incubation with 20 equiv. H<sub>2</sub>O<sub>2</sub>, but not with 100 equiv. H<sub>2</sub>O<sub>2</sub>. In the presence of a large excess amount of H<sub>2</sub>O<sub>2</sub> (>100 equiv.), the apparent deviation of the trace from single exponential curvature was observed, indicating that more complicated reactions occurred.

As the histidines in the Mb pocket are protonated at pH 5.1 and deprotonated at pH 7.4, the reaction rates of these Mb mutants were determined under pH 5.1 and 7.4. The rate constants  $k_{\text{obs}}$  were summarized in Table 2. The corresponding spectral changes were shown in Fig. 3 and Fig. S2–S9 (ESI†). From the reactions of Mn<sup>III</sup>Mbs (pH 7.4), we found that histidine at residue 64 plays a critical role to activate H<sub>2</sub>O<sub>2</sub>. Removal of His64, H64F Mn<sup>III</sup>Mb, replacing His64 with Phe, showed no reactivity. Even when the distal histidine was relocated to the positions of 43, or 29, or 43 and 29, the resulting Mn<sup>III</sup>Mbs showed little reactivity. Interestingly, F43H Mn<sup>III</sup>Mb, with two distal ligands (His43 and His 64), increases the reaction rate to 0.072 s<sup>−1</sup>, *ca.* 5-fold than that of wild type Mn<sup>III</sup>Mb. However, L29H Mn<sup>III</sup>Mb (His29 and His 64) showed few absorption spectra changes upon the addition of H<sub>2</sub>O<sub>2</sub>. Increasing the number of distal histidines to 3, the mutant L29H/F43H Mn<sup>III</sup>Mb exhibited a 2.4-fold higher reaction rate than that of wild-type Mn<sup>III</sup>Mb. Thus, L29H would inhibit the formation of Mn<sup>IV</sup>=O intermediate.

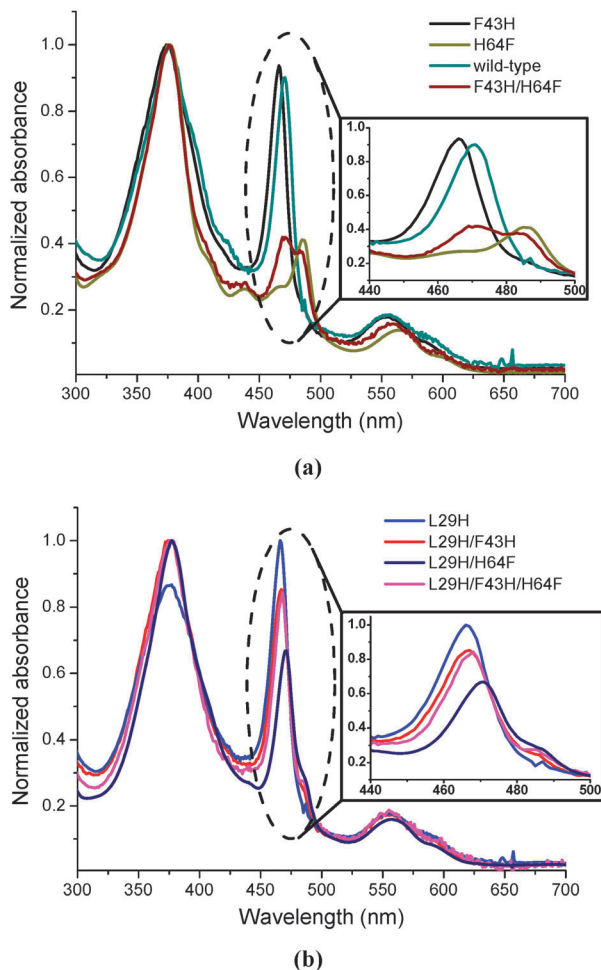


**Fig. 2** Normalized absorption spectra of (a) wild-type, F43H, H64F, F43H/H64F Mn<sup>III</sup>Mb and (b) L29H, L29H/F43H, L29H/H64F, L29H/F43H/H64F Mn<sup>III</sup>Mb mutants in 50 mM potassium phosphate buffer (pH 7.4). Insets: enlarged spectra from 440 to 500 nm.

**Table 2** Rate constants of different mutants with H<sub>2</sub>O<sub>2</sub>

Mb	Formation of metal-oxo ( $k_{\text{obs}}/\text{s}^{-1}$ )	
	Mn <sup>III</sup> Mb <sup>a</sup>	
	pH = 7.4	pH = 5.1
Wild-type	0.015	0.0078
L29H	N.D. <sup>b</sup>	N.D. <sup>b</sup>
F43H	0.072	N.D. <sup>b</sup>
H64F	N.D. <sup>b</sup>	N.D. <sup>b</sup>
L29H/F43H	0.036	N.D. <sup>b</sup>
L29H/H64F	N.D. <sup>b</sup>	N.D. <sup>b</sup>
F43H/H64F	N.D. <sup>b</sup>	N.D. <sup>b</sup>
L29H/F43H/H64F	N.D. <sup>b</sup>	N.D. <sup>b</sup>

<sup>a</sup> Reactions were performed with 29  $\mu\text{M}$  mutants and 580  $\mu\text{M}$  H<sub>2</sub>O<sub>2</sub> in 50 mM potassium phosphate buffer at 20 °C. <sup>b</sup> Reaction rates were too slow to measure.



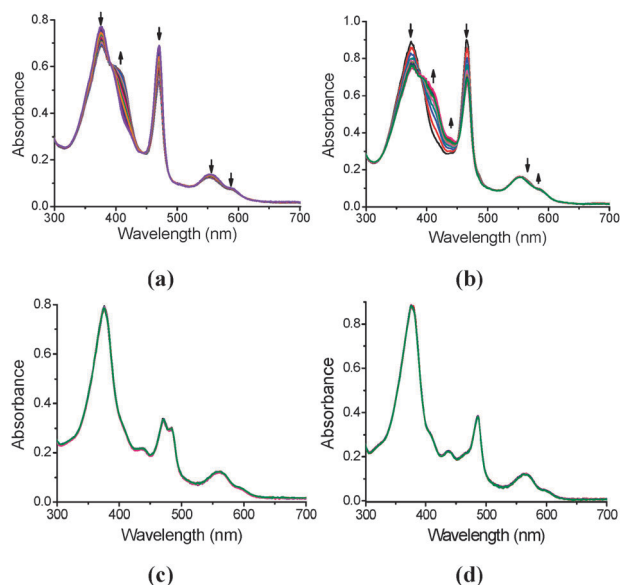


**Fig. 3** Spectral changes of (a) wild-type  $\text{Mn}^{\text{III}}\text{Mb}$ , (b) F43H  $\text{Mn}^{\text{III}}\text{Mb}$ , (c) F43H/H64F  $\text{Mn}^{\text{III}}\text{Mb}$  and (d) H64F  $\text{Mn}^{\text{III}}\text{Mb}$  mixing with  $\text{H}_2\text{O}_2$  at pH 7.4. The arrows in (a) and (b) indicate the directions of absorbance changes.

In addition, only wild type  $\text{Mn}^{\text{III}}\text{Mb}$  produced an  $\text{Mn}^{\text{IV}}=\text{O}$  intermediate in pH 5.1 and the reaction rate decreased to 0.5 fold that in pH 7.4, as shown in Table 2.

To better illustrate the dual histidines at the 64 and 43 positions accelerating the formation of  $\text{Mn}^{\text{IV}}=\text{O}$  intermediate, we plotted the time course ( $k_{\text{obs}}$ ), shown in Fig. 4, for the reactions of different mutated  $\text{Mn}^{\text{III}}\text{Mb}$ s (29  $\mu\text{M}$ ) with  $\text{H}_2\text{O}_2$  (580  $\mu\text{M}$ ) at pH 7.4, according to the changes of absorbance at 411 nm. This plot clearly showed that all mutants containing H64F didn't show  $\text{H}_2\text{O}_2$  reactivity, and only F43H and L29H/F43H exhibited higher reactivity than that of wild-type  $\text{Mn}^{\text{III}}\text{Mb}$ .

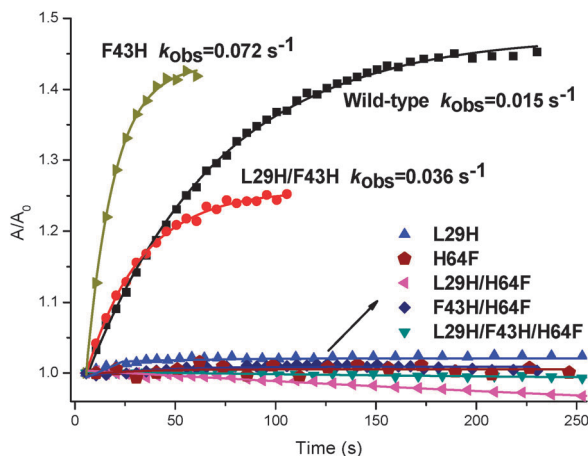


**Fig. 4** Time courses of  $\text{Mn}^{\text{IV}}=\text{O}$  por formation in the reaction with  $\text{H}_2\text{O}_2$  for different mutants.  $A/A_0$  refers to ratio of the absorbance and initial absorbance at 411 nm. Reaction conditions: mutants, 29  $\mu\text{M}$ ;  $\text{H}_2\text{O}_2$ , 580  $\mu\text{M}$  in 50 mM potassium phosphate buffer (pH 7.4) at 20  $^\circ\text{C}$ .

**Table 3** Reaction rates (turnover/min) of different mutants with ABTS and  $\text{H}_2\text{O}_2$  at pH 7.4

Mb	Rate (turnover $\text{min}^{-1}$ ) $\text{Mn}^{\text{III}}\text{Mb}^a$ pH = 7.4
Wild-type	0.023
L29H	0.0093
F43H	0.24
H64F	0.0012
L29H/F43H	0.15
L29H/H64F	0.0029
F43H/H64F	0.0017
L29H/F43H/H64F	0.018

<sup>a</sup> Reactions were performed with 29  $\mu\text{M}$  mutants, 580  $\mu\text{M}$  ABTS, and 580  $\mu\text{M}$   $\text{H}_2\text{O}_2$  in 50 mM potassium phosphate buffer at 20  $^\circ\text{C}$ .

### ABTS oxidation by $\text{Mn}^{\text{III}}\text{Mb}$ with $\text{H}_2\text{O}_2$

To examine the effect of distal histidine on the activity of  $\text{Mn}^{\text{III}}\text{Mb}$  as peroxidases, we chose 2,2'-azino-bis(3-ethylbenzthiazoline-6-sulphonic acid) (ABTS) as a probe because it serves as a colorimetric indicator for hypervalent metal porphyrin<sup>63–65</sup> or Salen species.<sup>66,67</sup> The experiments for ABTS oxidation were carried out at 20  $^\circ\text{C}$  with the ratio of the [catalyst]:[ $\text{H}_2\text{O}_2$ ]:[ABTS] being 29  $\mu\text{M}$ :580  $\mu\text{M}$ :580  $\mu\text{M}$  (1:20:20). The reaction rates (TOF, turnover  $\text{min}^{-1}$ ) were obtained by monitoring the change of absorption at 734 nm ( $\epsilon = 1.5 \times 10^4 \text{ M cm}^{-1}$ ). Table 3 summarizes the reaction rates of the  $\text{Mn}^{\text{III}}\text{Mb}$  mutants. F43H  $\text{Mn}^{\text{III}}\text{Mb}$  exhibited a  $\sim 10$  folds higher TOF than that of wild-type  $\text{Mn}^{\text{III}}\text{Mb}$  (0.023  $\text{min}^{-1}$ ). In contrast, the mutant L29H  $\text{Mn}^{\text{III}}\text{Mb}$  gave 0.5 fold lower TOF than wild-type  $\text{Mn}^{\text{III}}\text{Mb}$ . As expected, we could not find any significant activities for the  $\text{Mn}^{\text{III}}\text{Mb}$  containing H64F mutant, except for L29H/F43H/H64F which exhibited comparable reactivity to wild type  $\text{Mn}^{\text{III}}\text{Mb}$  for dual distal histidines. The changes in the TOF values correlate well with the reaction rates observed for the reactivities of  $\text{Mn}^{\text{III}}\text{Mb}$  with  $\text{H}_2\text{O}_2$ , following the trend: F43H > L29H/F43H > wild-type > F43H/L29H/H64F > L29H > H64F, L29H/H64F, F43H/H64F.

### Discussion

Previous studies for Mn substitution inside the protein scaffolds such as horseradish peroxidase ( $\text{Mn}^{\text{III}}\text{HRP}$ ), cytochrome-c peroxidase ( $\text{Mn}^{\text{III}}\text{CcP}$ ), microperoxidase-8 ( $\text{Mn}^{\text{III}}\text{MP-8}$ ) and myoglobin ( $\text{Mn}^{\text{III}}\text{Mb}$ ) showed the decrease of the reactivity toward  $\text{H}_2\text{O}_2$  and the related peroxidase activity.<sup>44,45,47–52</sup> This might be interpreted on the basis of unfavorable  $\text{H}_2\text{O}_2$  binding to the Mn center and the lower  $\text{pK}_a$  for  $\text{H}_2\text{O}_2$  deprotonation to a less extent than the Fe center. Thus, increasing the pH of aqueous media becomes an important approach to increase the reactivity of Mn porphyrins, inside or outside of protein scaffolds. Although the effects of the location of distal histidine on the reactivity of native heme toward  $\text{H}_2\text{O}_2$  inside myoglobin scaffold have been demonstrated by Watanabe and co-workers,<sup>22,56</sup> similar studies on the effect of the secondary coordination sphere on Mn reconstituted heme proteins have been seldom performed. Recently, Lu and coworkers reported the pH dependent

reactivity of an MnSalen cofactor, the analogue to Mn porphyrin, in myoglobin and demonstrated the effect of the distal ligand on binding, orienting and activating  $\text{H}_2\text{O}_2$ .<sup>33</sup> On the other hand, outside the protein scaffold, appending imidazole functional groups to the Salen or porphyrin ligand skeleton has been demonstrated to enhance their reactivity and selectivity toward oxidation. The imidazole functional groups are regarded as the distal or axial ligands to mimic the heme microenvironment in proteins.<sup>2,68</sup> Building on these initial successes, it is desirable to carry systematic studies for the effect of distal environment on  $\text{Mn}^{\text{III}}$  porphyrin at the defined locations inside myoglobin.

### Effect of distal histidine on water coordinating to Mn center

Absorption spectra of  $\text{Mn}^{\text{III}}$ Mb mutants revealed the ability of distal His64 to stabilize a water molecule around the Mn center. Although the Mn coordination mode in  $\text{Mn}^{\text{III}}$ Mb is still in debate, the crystal structure of  $\text{Mn}^{\text{III}}(\text{H}_2\text{O})\text{Mb}$  shows a mixture of a six-coordinate species (with axial water; 70% occupancy) and a five-coordinate species (without axial water; a non-bonded water refined to 30% in the distal pocket). Two conformations for the distal His64 residue refined to the corresponding 70% and 30% occupancies. Thus, this water is stabilized by hydrogen-bonding with the distal His64 residue. However, for the lower coordination ability of water to the Mn center, a five-coordinate species could also be observed, even though with a hydrogen bond forming between the distal His64 residue and water. Therefore, the mutant H64F MnMb showed the characteristic Soret band at 486 nm with low intensity, which might be assigned to be a five-coordinate  $\text{Mn}^{\text{III}}$  porphyrin.

Changing the location of the distal histidine from the 64 to 43 position, F43H/H64F  $\text{Mn}^{\text{III}}$ Mb showed a “split” of the second Soret band and an absorbance blue shift to 471 nm, indicating that the hydrophilicity of the distal environment increases. Another mutant L29H/H64F  $\text{Mn}^{\text{III}}$ Mb showed a blue shift of the second Soret band but with less intensity, compared with that of H64F  $\text{Mn}^{\text{III}}$ Mb, suggesting the distal histidine location resulted more hydrophilicity. This minor difference in the second Soret band may be explained by the crystal structures of L29H/H64L and F43H/H64L Mb, in which the distance between L29H and the water (2.67 Å) is shorter than that of F43H and water (2.75 Å).<sup>22</sup> Nevertheless, the distal histidine at 64 position could better stabilize a six-coordinate Mn por with an axial water than that at the 43 and 29 positions, which is different from the effect of the location of distal histidine residues on the heme-bound water in Mb mutants.

Interestingly, increasing distal histidine could facilitate a water binding Mn center and form a six-coordinate Mn porphyrin. From the absorption spectra of F43H, L29H, L29H/F43H and L29H/F43H/H64F Mb, we found a small blue shift (1–2 nm) of the second Soret band compared to the wild-type  $\text{Mn}^{\text{III}}$ Mb, suggesting the importance of hydrogen bond formation with distal His64 to water coordinating to the Mn center.

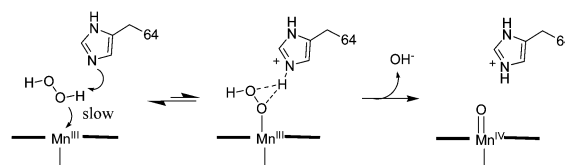
### Effect of distal histidine on the reaction with $\text{H}_2\text{O}_2$ activation

The reactivity of Mn por with  $\text{H}_2\text{O}_2$  is largely dependent on the existence, location and number of the distal histidine.

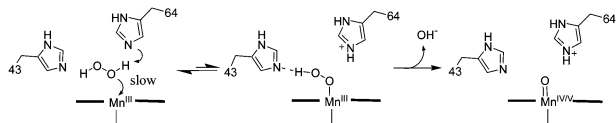
H64F  $\text{Mn}^{\text{III}}$ Mb with no distal histidine has no reactivity with  $\text{H}_2\text{O}_2$ . This is not surprising for low coordination ability of  $\text{H}_2\text{O}_2$  to Mn center in the absence of His64, which was previously observed in MnSalen inside H64F Mb.<sup>33</sup> Changing the locations of distal histidine from the 64 to 29 or/and 43 positions does not show the reactivity toward  $\text{H}_2\text{O}_2$ . Thus, it is apparent that His64 in wild-type Mb plays an essential role to enhance the reaction with  $\text{H}_2\text{O}_2$ , as shown in Scheme 1.

The mutation of Phe43 to His43, F43H  $\text{Mn}^{\text{III}}$ Mb, results in 5-fold higher reactivity than wild-type  $\text{Mn}^{\text{III}}$ Mb; whereas L29H  $\text{Mn}^{\text{III}}$ Mb showed no reactivity. This indicates that an appropriate choice of the second distal histidine is important to the acceleration of the O–O bond cleavage of the Mn-bound peroxide. From the crystal structures of the ferric L29H/H64L, F43H/H64L Mb and wild-type Mb, we found that the distance of His29 from the metal ion center is *ca.* 6.6 Å, which is farther from the Mn porphyrin than that of His43 (5.7 Å) and His64 (4.3 Å). This indicates that His29 in the mutant facilitates the reaction less efficiently than His64 and His43 in wild-type and F43H Mb. For the F43H mutant, the distal His43 has a similar distance from the heme iron compared with peroxidases and could form a hydrogen bond with the  $\text{H}_2\text{O}_2$  coordinated to the Mn center, which may enhance the O–O bond cleavage and showed a *ca.* 5-fold rate increase in the reaction with  $\text{H}_2\text{O}_2$  versus wild-type  $\text{Mn}^{\text{III}}$ Mb. For the short distance to the Mn center, His64 makes a direct hydrogen bond with the Mn-bound  $\text{H}_2\text{O}_2$ , which stabilizes the coordination of  $\text{H}_2\text{O}_2$ . However, for the possible interaction of the distal histidine between both oxygen atoms of the Mn-bound peroxide, His64 does not facilitate the charge separation, as suggested for the role of the wild-type Mb.<sup>56</sup> Thus, as shown in Scheme 2, for Mn reconstituted Mb, His64 is critical to bind  $\text{H}_2\text{O}_2$  and His43 facilitates the activation of  $\text{H}_2\text{O}_2$  as a base to promote the O–O bond cleavage.

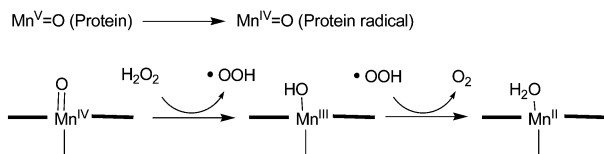
This cooperative effect of dual distal histidines had not been observed in the reaction between iron and  $\text{H}_2\text{O}_2$  in native Mb and the mutated Mbs.<sup>56</sup> The difference between  $\text{Fe}^{\text{III}}$ Mb and  $\text{Mn}^{\text{III}}$ Mb was supposed due to the different coordination and deprotonation abilities of  $\text{H}_2\text{O}_2$  coordinated to  $\text{Fe}^{\text{III}}$  and  $\text{Mn}^{\text{III}}$ . Harriman and co-workers have reported the first  $\text{pK}_a$  of coordinated water for  $\text{Fe}^{\text{III}}$  and  $\text{Mn}^{\text{III}}$  porphyrin complexes as 6.6 and 8.0, respectively.<sup>69</sup> In the protein scaffold, the same order has been reported by Veeger and coworkers.<sup>50</sup> The  $\text{pK}_a$  of metal-bound water for  $\text{Mn}^{\text{III}}$ MP-8 was 11.2, two units higher than that for  $\text{Fe}^{\text{III}}$ MP-8 ( $\text{pK}_a = 9.2$ ). The higher  $\text{pK}_a$  for  $\text{Mn}^{\text{III}}$  indicated that  $\text{H}_2\text{O}$  deprotonated with more difficulty when it is coordinated



**Scheme 1** The proposed mechanism of  $\text{Mn}^{\text{IV}}=\text{O}$  porphyrin formation and possible interactions between His64 and hydrogen peroxide in wild-type  $\text{Mn}^{\text{III}}$ Mb.



**Scheme 2** The proposed mechanism of  $\text{Mn}^{\text{IV}}=\text{O}$  por formation and possible interactions between His-43/His-64 and hydrogen peroxide in F43H mutant.



**Scheme 3** The proposed mechanism of  $\text{Mn}^{\text{II}}$  por formation from high valent  $\text{Mn}^{\text{IV}}$  or  $\text{Mn}^{\text{V}}$  species in the presence of large excess amount of  $\text{H}_2\text{O}_2$ .

to  $\text{Mn}^{\text{III}}$  than to  $\text{Fe}^{\text{III}}$ . Similar to  $\text{H}_2\text{O}$ , we proposed that the deprotonation of  $\text{H}_2\text{O}_2$  is important to coordinate to  $\text{Mn}^{\text{III}}$ . It had been reported that the coordination of  $\text{H}_2\text{O}_2$  to  $\text{Mn}^{\text{III}}\text{Mb}$  was less favorable than that to  $\text{Fe}^{\text{III}}\text{Mb}$ ,<sup>52</sup> which supports our consideration.

### Effect of distal histidine on peroxidase activity

The peroxidase activities of  $\text{Mn}^{\text{III}}\text{Mb}$  were measured for the 1-electron oxidation of ABTS, which roughly correlates with the reactivities of  $\text{Mn}^{\text{III}}\text{Mbs}$  with  $\text{H}_2\text{O}_2$  (Tables 1 and 2). However, the 10-fold increase in F43H  $\text{Mn}^{\text{III}}\text{Mb}$  versus wild-type  $\text{Mn}^{\text{III}}\text{Mb}$  is greater than the 5-fold improvement in the reactivity of the F43H Mb with  $\text{H}_2\text{O}_2$ . Given the fast reaction between ABTS with high valent  $\text{Mn}^{\text{IV}}$  or  $\text{Mn}^{\text{V}}$  intermediates through one-electron oxidation in the presence of a large excess amount of the substrates, the rate-determining step for the one-electron oxidation is the formation of high valent  $\text{Mn}^{\text{IV}}$  or  $\text{Mn}^{\text{V}}$  intermediates. Thus, the difference between the reaction rates with  $\text{H}_2\text{O}_2$  and one-electron oxidation of ABTS indicates the possibility of reactivity of  $\text{H}_2\text{O}_2$  with high valent  $\text{Mn}^{\text{IV}}$  or  $\text{Mn}^{\text{V}}$  intermediates. Indeed, in the presence of a large excess amount of  $\text{H}_2\text{O}_2$  (>100 equiv.), we observed the formation of  $\text{Mn}^{\text{II}}$  species in UV-vis spectra, which exhibit the absorption at 440 nm for the F43H mutant (seen in Fig. S1, ESI†). In accordance with the previous reports for  $\text{Mn}^{\text{V}}=\text{O}$  (ref. 70) and  $\text{Fe}^{\text{IV}}=\text{O}$  in protein scaffolds with excess  $\text{H}_2\text{O}_2$ ,<sup>71</sup> we proposed the mechanism of  $\text{Mn}^{\text{II}}$  formation as described in Scheme 3.

## Conclusions

In summary, we have prepared L29H, F43H, H64F, L29H/H64F, F43H/H64F, L29H/F43H and L29H/F43H/H64F mutants to clarify the effects of distal histidines to activate  $\text{H}_2\text{O}_2$  by Mn protoporphyrin IX. The modulation of distal environment is achieved through hydrogen bonding interactions by the distal ligand through perturbation of  $\text{H}_2\text{O}_2$  protonation/deprotonation equilibrium. Distal histidine at the 64 position plays an essential role to bind  $\text{H}_2\text{O}_2$  through hydrogen bonding formation, which facilitates the coordination of  $\text{H}_2\text{O}_2$  to Mn center.

The second distal at the 43 position is important for cleavage of the O–O bond and forming the high valent Mn-oxo intermediate. This cooperative effect of dual distal histidines on the activation of  $\text{H}_2\text{O}_2$  by Mn porphyrin inside protein scaffold is firstly observed. As a consequence, through tuning the distal histidine to bind and orient  $\text{H}_2\text{O}_2$ , the reactivity to activate  $\text{H}_2\text{O}_2$  exhibits significant changes. The F43H  $\text{Mn}^{\text{III}}\text{Mb}$  mutant exhibited 5-fold and 10-fold increases in reaction rates in the activation of  $\text{H}_2\text{O}_2$  and one-electron oxidation of ABTS versus wild-type  $\text{Mn}^{\text{III}}\text{Mb}$ . In our group, we will continue to investigate the activation of reactive oxygen species (ROS) by metal porphyrins through modulating the secondary coordination spheres of protein scaffolds, which would help us to understand the “trick” of nature to activate small molecules and further provide new insights to develop biomimetic catalysis.

## Experimental section

### General

Chemicals such as protoporphyrin IX,  $\text{H}_2\text{O}_2$ , and ABTS were purchased from Alfa Aesar and used without further purification. Manganese(III) protoporphyrin IX was prepared according to the reported method.<sup>45,72</sup> ESI-MS spectra were recorded with Bruker Apex IV FTMS spectrometer. UV-vis spectra were recorded with Agilent 8453 UV-Vis spectrometer.

### Preparation of proteins

Mutations at desired locations were introduced *via* a polymerase chain reaction-based technique. Heme proteins were purified as described in previous reports.<sup>33,59,73</sup> The extraction of heme and reconstitution of manganese(III) protoporphyrin IX to apo-myoglobin were according to the literature.<sup>36,51,60–62</sup> All mutants were verified by ESI-MS.

### Kinetic studies with $\text{H}_2\text{O}_2$

The reactions were initiated by 20 equiv.  $\text{H}_2\text{O}_2$  in 50 mM potassium phosphate buffer, detected by UV-vis spectrometer. In the reaction, 580  $\mu\text{M}$   $\text{H}_2\text{O}_2$  was added to 29  $\mu\text{M}$  protein solution, the reaction temperature was 20 °C. The kinetic traces at 411 nm for  $\text{Mn}^{\text{IV}}=\text{O}$  Por were used for calculating the pseudo first-order rates  $k_{\text{obs}}$  by fitting to a single-exponential eqn (1):

$$y = y_0 + a(1 - e^{-x/t}) \quad (1)$$

where  $x$  is reaction time, and  $y$  is the absorbance at  $\lambda = 424$  nm.  $k_{\text{obs}} = -1/t$ .

### ABTS oxidation

Proteins were mixed with 20 equiv. ABTS in 50 mM potassium phosphate buffer. The reactions were initiated by adding 20 equiv.  $\text{H}_2\text{O}_2$ , monitored at 734 nm with a UV-vis spectrometer. Reaction conditions: 29  $\mu\text{M}$  protein, 580  $\mu\text{M}$  ABTS, and 580  $\mu\text{M}$   $\text{H}_2\text{O}_2$  was mixed at 20 °C. The turnover numbers for ABTS were calculated at 734 nm ( $\epsilon = 1.5 \times 10^4 \text{ M cm}^{-1}$  for  $\text{ABTS}^{\bullet+}$ ).<sup>74</sup>

## Acknowledgements

This project was supported by National Scientific Foundation of China (grant no. 20971007 and 21101169), National Key Basic Research Support Foundation of China (NKBRSCF) (2010CB912302), and SRFDP (20090001110029). X.-H. Li thanks National Funding for Fostering Talents of Basic Sciences (J0630421).

## Notes and references

- 1 A. Werner, *Justus Liebigs Ann. Chem.*, 1912, **386**, 1.
- 2 R. L. Shook and A. S. Borovik, *Inorg. Chem.*, 2010, **49**, 3646.
- 3 A. Werner, *Neuere Anschauungen auf dem Gebiete der anorganischen Chemie*, Vieweg und Sohn, Braunschweig, 3rd edn, 1913.
- 4 I. Bertini, H. B. Gray, S. J. Lippard and J. S. Valentine, *Bioinorganic Chemistry*, University Science Books, Mill Valley, CA, 1994.
- 5 S. J. Lippard and J. M. Berg, *Principles of Bioinorganic Chemistry*, University Science Books, Mill Valley, CA, 1994.
- 6 J. H. Dawson, *Science*, 1988, **240**, 433.
- 7 P. R. Ortiz de Montellano, *Acc. Chem. Res.*, 1987, **20**, 289.
- 8 A. S. Borovik, *Acc. Chem. Res.*, 2005, **38**, 54.
- 9 J. Geng, K. Dornevil and A. Liu, *J. Am. Chem. Soc.*, 2012, **134**, 12209.
- 10 Y. Lu, N. Yeung, N. Sieracki and N. M. Marshall, *Nature*, 2009, **460**, 855.
- 11 M. Unno, T. Matsui and M. Ikeda-Saito, *J. Inorg. Biochem.*, 2012, **113**, 102.
- 12 R. H. Holm and E. I. Solomon, *Chem. Rev.*, 2004, **104**, 247.
- 13 Y. Lu and J. S. Valentine, *Curr. Opin. Struct. Biol.*, 1997, **7**, 495.
- 14 Y. Lu, S. M. Berry and T. D. Pfister, *Chem. Rev.*, 2001, **101**, 3047.
- 15 J. M. Matthews, F. E. Loughlin and J. P. Mackay, *Curr. Opin. Struct. Biol.*, 2008, **18**, 484.
- 16 N. Yeung, Y.-W. Lin, Y.-G. Gao, X. Zhao, B. S. Russell, L. Lei, K. D. Miner, H. Robinson and Y. Lu, *Nature*, 2009, **462**, 1079.
- 17 Z. N. Zahran, L. Chooback, D. M. Copeland, A. H. West and G. B. Richter-Addo, *J. Inorg. Biochem.*, 2008, **102**, 216.
- 18 Y.-W. Lin, N. Yeung, Y.-G. Gao, K. D. Miner, S. Tian, H. Robinson and Y. Lu, *Proc. Natl. Acad. Sci. U. S. A.*, 2010, **107**, 8581.
- 19 S. Ozaki, M. P. Roach, T. Matsui and Y. Watanabe, *Acc. Chem. Res.*, 2001, **34**, 818.
- 20 J. L. Bourassa, E. P. ves, A. L. Marqueling, R. Shimanovich and J. T. Groves, *J. Am. Chem. Soc.*, 2001, **123**, 5142.
- 21 S. Ozaki, T. Matsui and Y. Watanabe, *J. Am. Chem. Soc.*, 1996, **118**, 9784.
- 22 S. Ozaki, T. Matsui, M. P. Roach and Y. Watanabe, *Coord. Chem. Rev.*, 2000, **198**, 39.
- 23 J.-L. Primus, M. G. Boersma, D. Mandon, S. Boeren, C. Veeger, R. Weiss and I. M. C. M. Rietjens, *JBIC, J. Biol. Inorg. Chem.*, 1999, **4**, 274.
- 24 N. Yeung and Y. Lu, *Chem. Biodiversity*, 2008, **5**, 1437.
- 25 Y. Lu, *Angew. Chem., Int. Ed.*, 2006, **45**, 5588.
- 26 E. S. Ryabova and E. Nordlander, *Dalton Trans.*, 2005, 1228.
- 27 D. W. Low, S. Abedin, G. Yang, J. R. Winkler and H. B. Gray, *Inorg. Chem.*, 1998, **37**, 1841.
- 28 T. M. Makris, K. Koenig, I. Schlichting and S. G. Sligar, *J. Inorg. Biochem.*, 2006, **100**, 507.
- 29 S. Kato, T. Ueno, S. Fukuzumi and Y. Watanabe, *J. Biol. Chem.*, 2004, **279**, 52376.
- 30 H.-S. Park, S.-H. Nam, J. K. Lee, C. N. Yoon, B. Mannervik, S. J. Benkovic and H.-S. Kim, *Science*, 2006, **311**, 535.
- 31 Y. Lu, *Curr. Opin. Chem. Biol.*, 2005, **9**, 118.
- 32 T. Hayashi and Y. Hisaeda, *Acc. Chem. Res.*, 2002, **35**, 35.
- 33 J.-L. Zhang, D. K. Garner, L. Liang, D. A. Barrios and Y. Lu, *Chem.-Eur. J.*, 2009, **15**, 7481.
- 34 J. Steinreiber and T. R. Ward, *Coord. Chem. Rev.*, 2008, **252**, 751.
- 35 M. Ohashi, T. Koshiyama, T. Ueno, M. Yanase, H. Fujii and Y. Watanabe, *Angew. Chem., Int. Ed.*, 2003, **42**, 1005.
- 36 J. R. Carey, S. K. Ma, T. D. Pfister, D. K. Garner, H. K. Kim, J. A. Abramite, Z. Wang, Z. Guo and Y. Lu, *J. Am. Chem. Soc.*, 2004, **126**, 10812.
- 37 J.-L. Zhang, D. K. Garner, L. Liang, Q. Chen and Y. Lu, *Chem. Commun.*, 2008, 1665.
- 38 D. K. Garner, L. Liang, D. A. Barrios, J.-L. Zhang and Y. Lu, *ACS Catal.*, 2011, **1**, 1083.
- 39 T. Hayashi, D. Murata, M. Makino, H. Sugimoto, T. Matsui, H. Sato, Y. Shiro and Y. Hisaeda, *Inorg. Chem.*, 2006, **45**, 10530.
- 40 J. Barber and J. W. Murray, *Coord. Chem. Rev.*, 2008, **252**, 233.
- 41 H. Dau and M. Haumann, *Coord. Chem. Rev.*, 2008, **252**, 273.
- 42 S. Signorella and C. Hureau, *Coord. Chem. Rev.*, 2012, **256**, 1229.
- 43 V. Daier, D. Moreno, C. Duhayon, J.-P. Tuchagues and S. Signorella, *Eur. J. Inorg. Chem.*, 2010, 965.
- 44 R. J. Nick, G. B. Ray, K. M. Fish, T. G. Spiro and J. T. Groves, *J. Am. Chem. Soc.*, 1991, **113**, 1838.
- 45 K. K. Khan, M. S. Mondal and S. Mitra, *J. Chem. Soc., Dalton Trans.*, 1996, 1059.
- 46 K. K. Khan, M. S. Mondal and S. Mitra, *J. Chem. Soc., Dalton Trans.*, 1998, 533.
- 47 X. Wang and Y. Lu, *Biochemistry*, 1999, **38**, 9146.
- 48 A. Gengenbach, S. Syn, X. Wang and Y. Lu, *Biochemistry*, 1999, **38**, 11425.
- 49 C. Veeger, *J. Inorg. Biochem.*, 2002, **91**, 35.
- 50 J.-L. Primus, S. Grunenwald, P.-L. Hagedoorn, A.-M. Albrecht-Gary, D. Mandon and C. Veeger, *J. Am. Chem. Soc.*, 2002, **124**, 1214.
- 51 M. S. Mondal, S. Mazumdar and S. Mitra, *Inorg. Chem.*, 1993, **32**, 5362.
- 52 M. S. Mondal and S. Mitra, *Biochim. Biophys. Acta, Protein Struct. Mol. Enzymol.*, 1996, **1296**, 174.
- 53 J. R. Lindsay Smith, P. N. Balasubramanian and T. C. Bruice, *J. Am. Chem. Soc.*, 1988, **110**, 7411.
- 54 K. Murata, R. Panicucci, E. Gopinath and T. C. Bruice, *J. Am. Chem. Soc.*, 1990, **112**, 6072.
- 55 R. D. Arasasingham and T. C. Bruice, *J. Am. Chem. Soc.*, 1991, **113**, 6095.



- 56 T. Matsui, S. Ozaki, E. Liong, G. N. Phillips, Jr. and Y. Watanabe, *J. Biol. Chem.*, 1999, **274**, 2838.
- 57 T. Matsui, S. Ozaki and Y. Watanabe, *J. Am. Chem. Soc.*, 1999, **121**, 9952.
- 58 S. Ozaki, I. Hara, T. Matsui and Y. Watanabe, *Biochemistry*, 2001, **40**, 1044.
- 59 J. L. Anderson, J. Ding, R. D. McCulla, W. S. Jenks and D. W. Armstrong, *J. Chromatogr., A*, 2002, **946**, 197.
- 60 B. A. Springer and S. G. Sligar, *Proc. Natl. Acad. Sci. U. S. A.*, 1987, **84**, 8961.
- 61 F. W. J. Teale, *Biochim. Biophys. Acta*, 1959, **35**, 543.
- 62 W. R. Fisher, H. Taniuchi and C. B. Anfinsen, *J. Biol. Chem.*, 1973, **248**, 3188.
- 63 T. C. Bruice, P. N. Balasubramanian, R. W. Lee and J. R. L. Smith, *J. Am. Chem. Soc.*, 1988, **110**, 7890.
- 64 R. D. Arasasingham, S. Jeon and T. C. Bruice, *J. Am. Chem. Soc.*, 1992, **114**, 2536.
- 65 T. C. Bruice, M. F. Zippies and W. A. Lee, *Proc. Natl. Acad. Sci. U. S. A.*, 1986, **83**, 4646.
- 66 M. Maneiro, M. R. Bermejo, M. I. Fernandez, E. Gomez-Forneas, A. M. Gonzalez-Noya and A. M. Tytyshkin, *New J. Chem.*, 2003, **27**, 727.
- 67 M. R. Bermejo, M. I. Fernandez, A. M. Gonzalez-Noya, M. Maneiro, R. Pedrido, M. J. Rodriguez, J. C. Garcia-Monteagudo and B. Donnadieu, *J. Inorg. Biochem.*, 2006, **100**, 1470.
- 68 R. Li, J. Tian, H. Liu, S. Yan, S. Guo and J. Zhang, *Transition Met. Chem.*, 2011, **36**, 811.
- 69 A. Harriman and G. Porter, *J. Chem. Soc., Faraday Trans. 2*, 1979, **75**, 1532.
- 70 N. Jin, D. E. Lahaye and J. T. Groves, *Inorg. Chem.*, 2010, **49**, 11516.
- 71 J. J. Braymer, K. P. O'Neill, J.-U. Rohde and M. H. Lim, *Angew. Chem., Int. Ed.*, 2012, **51**, 5376.
- 72 T. Yonetani and T. Asakura, *J. Biol. Chem.*, 1969, **244**, 4580.
- 73 J. A. Sigman, B. C. Kwok and Y. Lu, *J. Am. Chem. Soc.*, 2000, **122**, 8192.
- 74 R. Re, N. Pellegrini, A. Proteggente, A. Pannala, M. Yang and C. Rice-Evans, *Free Radical Biol. Med.*, 1999, **26**, 1231.